+ *

Scanning band topology by the modulation instability

A. Maluckov[+,*]

D. Leykam[*o], D. Smirnova[x], S. Flach[*], E. Smolina[#]

x

o

#

Synergy of topology and nonlinearity either inherently present or activated in photonic systems opens new gates for fundamental science and discoveries of new functionalities of the devices [1]. **We are challenged by the sensitivity of the band topology to the modulation instability [2] and vice versa, related bulk-edge correspondence and nonlinearity driven topological phase transitions in photonic lattices** [3]. Here, our first findings in this emerging field will be briefly presented.

References
[1] D. Smirnova, D. Leykam, Y. D. Chong, and Y. Kivshar, Nonlinear topological photonics, Appl. Phys. Rev. 7, 021306 (2020).
[2] V. E. Zakharov, L. A. Ostrovsky, Physica 238D, 540 (2009).
[3] D. Leykam, E. Smolina, A. Maluckov, S. Flach, D. A. Smirnova, PRL 126, 073901 (2021).

Primary goal:

Probing the band topology by the modulation instability (MI).

Founded on the MI underlying mechanism: the energy dependent parametric gain which can enable selective population of a single Bloch band starting from a simple plane wave initial state.

Peculiarity: band topological properties measurement require absence of interband mixing in the system

Previous approaches [4]: Bloch band tomography
bulk-edge correspondence

Our approach: nonlinear dynamics of Bloch waves and related MI

References
[4] S. Mittal, S. Ganeshan, J. Fan, A. Vaezi, M. Hafezi, Nat. Photonics 10, 180 (2016); C.-E. Bardyn, S. D. Huber, O. Zilberberg, New J. Phys. 16, 123013 (2014).

Talk overview:

I **Brief introduction in topological 2D lattices**

Topological invariants: band Chern number and edge modes
Polarization vs. Chern number

II **Nonlinear dynamics of Bloch waves sensitivity to band topology**

the short time dynamics (linear stability analysis, LSA)
high symmetry points of the Brillouin zone (Dirac model)
the long time dynamics (direct numerical simulations)

III **Conclusions**

I Brief introduction in topological 2D lattices [5]

Topological band structures are a ubiquitous property of waves inside a periodic medium, regardless of the classical or quantum nature of the waves.

Topological photonics is a rapidly emerging field of research in which geometrical and topological ideas are exploited to design and control the behavior of light.

Breakthrough → Electromagnetic waves in 2D spatially periodic devices embedding time-reversal-breaking magneto-optical elements providing the photonic bands with non-trivial topological invariants [6].

The relationship: bulk topological invariant (Chern number) and the number of localized edge modes → the bulk-edge correspondence [7]←→

The sum of the Chern numbers associated with the occupied bulk bands is equal to the number of edge modes contributing to the edge current

Topological phase transitions → band gap opening after the PT symmetry breaking at Dirac points → nonzero Berry curvature and Chern number [5,6]

References
[5] T. Ozawa, H. M. Price, A. Amo, N. Goldman, M. Hafezi, L. Lu, M. C. Rechtsman, D. Schuster, J.Simon, O.Zilberberg, I. Carusotto, Rev. Mod. Phys. 91, 015006 (2019).
[6] F. D. M. Haldane, S. Raghu, Physical Review Letters 100, 013904 (2008). S. Raghu, F. D. M. Haldane Physical Revview A 78,033834 (2008)
[7] J. K. Asbóth, L. Oroszlány, A. Pályi, A short course on topological insulators (2016).

π- flux square lattice [2,8,9]

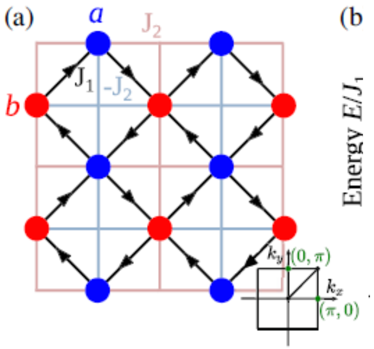

Fig. 1 Δ -detuning between sublattices
$J_{1,2}$ – NN and NNN hopping strengths

$$\widehat{H}_L(\vec{k}) = \vec{d}(\vec{k}) \cdot \vec{\sigma} \quad (1)$$

$$d_z = \Delta + 2J_2(\cos k_x - \cos k_y),$$

$$d_x + id_y = J_1\left(e^{-\frac{i\pi}{4}}\left(1 + e^{i(k_y - k_x)}\right) + e^{\frac{i\pi}{4}}(e^{-ik_x} + e^{ik_y}) \quad \right)$$

$$\hat{H}_L(\boldsymbol{k})\,|u_\pm(\boldsymbol{k})\rangle = E_\pm(\boldsymbol{k})\,|u_\pm(\boldsymbol{k})\rangle \quad (2)$$

$$E_\pm = \pm|d| = \pm\sqrt{d_x^2 + d_y^2 + d_z^2} \quad (3)$$

References
[8] T. Neupert, L. Santos, C. Chamon, C. Mudry, Phys. Rev. Lett. 106,236804 (2011).
[9] D. Leykam, E. Smolina, A. Maluckov, S. Flach, D. A. Smirnova, Supplement to PRL 126, 073901 (2021).

$$E_{\pm}(k,\Delta)=\pm\sqrt{4J_1^2\left[1+\cos k_x\cos k_y\right]+\left(\Delta+2J_2\left(\cos k_x-\cos k_y\right)\right)^2}$$

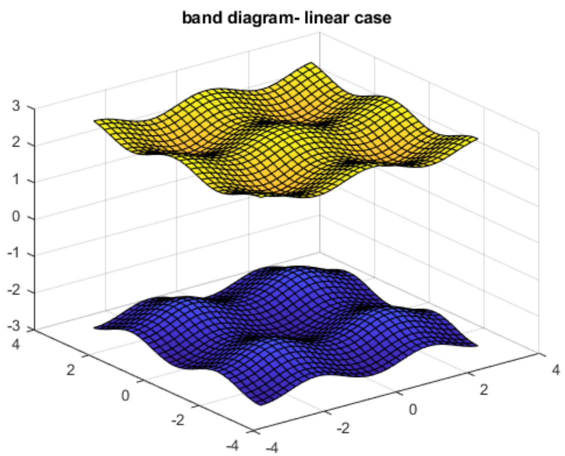

Fig2. (a) $J_2=J_1/\sqrt{2}$ *,* $\Delta=0$ *(max flatness)*

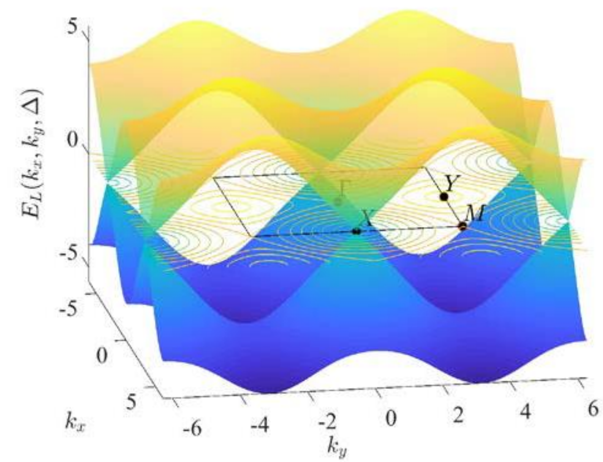

Fig. 2 (*b*) $J_1=1, J_2=\frac{J_1}{2}$, $\Delta=2\sqrt{2}J_1$

* Checking done for: the Bernevig–Hughes–Zhang Model (BHZ), Haldane model

Band topological invariant – Chern number: $$C_{\pm} = \frac{1}{2\pi} \iint_{BZ} \mathcal{F}_{\pm}(\boldsymbol{k}) \mathrm{d}^2\boldsymbol{k}, \qquad (4)$$

Berry curvature: $$\mathcal{F}_{\pm}(\boldsymbol{k}) = i\left[\langle \partial_{k_x} u_{\pm} | \partial_{k_y} u_{\pm} \rangle - \langle \partial_{k_y} u_{\pm} | \partial_{k_x} u_{\pm} \rangle\right] \qquad (5)$$

$\hat{\boldsymbol{n}}$ – a real unit polarization vector on the surface of Bloch sphere [10]:

$$\boldsymbol{d} \cdot \langle u_{\pm} | \hat{\boldsymbol{\sigma}} | u_{\pm} \rangle = E_{\pm} = \pm |\boldsymbol{d}| \Rightarrow \hat{\boldsymbol{n}}_{\pm} \equiv \langle u_{\pm} | \hat{\boldsymbol{\sigma}} | u_{\pm} \rangle = \pm \boldsymbol{d}/|\boldsymbol{d}| \qquad (6)$$

$$\mathcal{F}_{\pm} = \pm \boldsymbol{d}/|\boldsymbol{d}|^3$$

$$\mathcal{F}_{\pm}(\boldsymbol{k}) = -\frac{1}{2}\hat{\boldsymbol{n}}_{\pm} \cdot \left[(\partial_{k_x} \hat{\boldsymbol{n}}_{\pm}) \times (\partial_{k_y} \hat{\boldsymbol{n}}_{\pm})\right] \qquad (7)$$

Quantized $C_{\pm}$ change only at topological transitions where the band gap closes

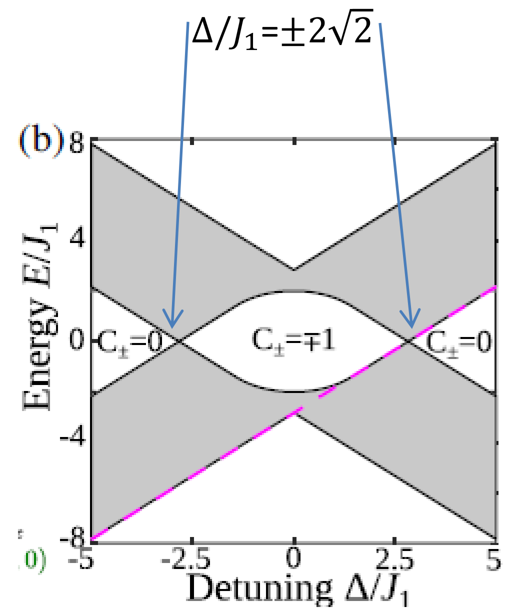

Fig. 3 Linear bands: $J_2 = J_1/\sqrt{2}$

References

[10] T. Fosel, V. Peano, F. Marquardt, New. J. Phys. 19, 115013 (2017).

II MI of NL Bloch waves

(a) The short time dynamics

- preparation of conditions for intra-band mixing

$$i\partial_t|\psi(\vec{r},t)>=(\widehat{H}_L+\widehat{H}_{NL})|\psi(\vec{r},t)> \tag{8}$$

$$\widehat{H}_{NL}=\Gamma diag[f(|\psi_a(\vec{r})|^2),f(|\psi_b(\vec{r})|^2)] \tag{9}$$

The linear Bloch wave (BW) can be continued as a nonlinear BW $|\phi(\boldsymbol{r})\rangle=(\sqrt{I_0},0)^T e^{i\pi x}$

Satisfying $(\widehat{H}_L+\widehat{H}_{NL})|\phi>=E_{NL}\,|\phi>$ with energy $E_{NL}=\Delta-4J_2+\Gamma f(I_0)$

LSA: nl Bloch mode (steady state) + small perturbation

$$|\psi(\boldsymbol{r},t)\rangle=(|\phi(\boldsymbol{r})\rangle+|\delta\phi(\boldsymbol{r},t)\rangle)e^{-iEt} \tag{10}$$

Linearized evolution equation for perturbations

$$(i\partial_t+E)|\delta\phi(\boldsymbol{r},t)\rangle=\widehat{H}_L|\delta\phi(\boldsymbol{r},t)\rangle+\Gamma\sum_{j=a,b}\left[\left(f(|\phi_j|^2)+f'(|\phi_j|^2)|\phi_j|^2\right)\delta\phi_j(\boldsymbol{r},t)+f'(|\phi_j|^2)|\phi_j|^2\delta\phi^*{}_j(\boldsymbol{r},t)\right]|j>$$

$$|\delta\phi(\boldsymbol{r},t)\rangle=|w(\boldsymbol{r})\rangle\,e^{-i\lambda t}+|v^*(\boldsymbol{r})\rangle\,e^{i\lambda^* t} \tag{11}$$

Cubic and saturable nl are considered: f(I)=I*, $f(I)=2I/(1+I)$

The eigenvalue problem of small perturbations:

Assumption for steady state : $|\phi(\boldsymbol{r})\rangle = |\phi\rangle\, e^{i\boldsymbol{k_0}\cdot\boldsymbol{r}}$ (12)

+ Fourier transformation

$$\lambda\,|w(\boldsymbol{k}+\boldsymbol{k}_0)\rangle = (\hat{H}(\boldsymbol{k}_0+\boldsymbol{k}) - E)\,|w\rangle + \Gamma \sum_{j=a,b,\ldots} \left[(f(|\phi_j|^2) + f'(|\phi_j|^2)|\phi_j|^2])w_j + f'(|\phi_j|^2)\phi_j^2 v_j\right]|j\rangle\,,$$

$$\lambda\,|v(\boldsymbol{k}-\boldsymbol{k}_0)\rangle = -(\hat{H}^*(\boldsymbol{k}_0-\boldsymbol{k}) - E)\,|v\rangle - \Gamma \sum_{j=a,b,..} \left[(f(|\phi_j|^2) + f'(|\phi_j|^2)|\phi_j|^2])w_j + f'(|\phi_j|^2)\phi_j^{*2} w_j\right]|j\rangle$$

(13)

Particle – hole symmetry :
Eigenvalues λ occur in complex conjugate pairs;

real λ -- stable perturbation modes,
Pure Imaginary – exponential instability,
complex – oscillatory instability

Example: weak nonlinearity limit Γ<<1, nl Bloch wave

$$|\phi\rangle = (\sqrt{I_0}, 0),\ d_{x,y}(k_0) = 0,\ d_z(k_0) = \Delta - 4J_2 \tag{14}$$
$$\vec{k} = 0$$

$$\lambda = 0, 0, \pm[2d_z(k_0) + \Gamma f(I_0)] \quad \text{a 4-fold degeneracy when} \quad \Gamma I_0 = -m_{eff}, \tag{15}$$
$$m_{eff} = \Delta - 4J_2$$

-Critical (stable) line at $\Gamma I_0/2 = -m_{eff}$: nl energy shift on *a*-sublattice closes the band gap and separates the region of exponential from complex instability (Fig. 4)

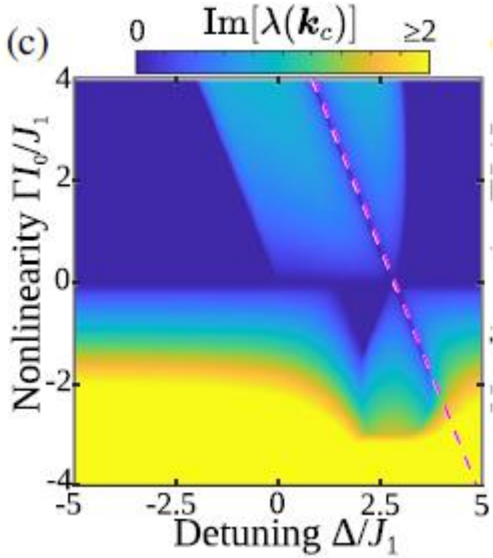

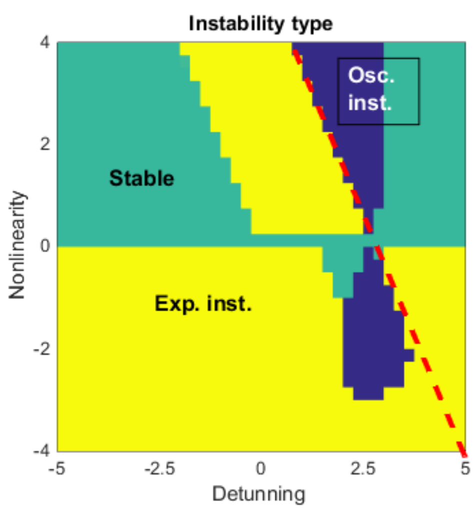

Fig. 4

(b) The high symmetry points of the Brillouin zone

Stability window of BWs at a critical nonlinearity strength $\Gamma I_0/2 = -m_{eff}$

The critical strength coincides with the bifurcation of a nonlinear Dirac cone [11];

Brief note: **The effective Dirac model** is obtained as a long wavelength expansion of Eq. (1)

$$\vec{k} = \vec{k}_0 + \vec{p}, |\vec{p}| \ll 1$$

$$\hat{H}_D = J_1\sqrt{2}\left(p_x\hat{\sigma}_y - p_y\hat{\sigma}_x\right) + (m_{eff} + J_2\left[{p_x}^2 + {p_y}^2\right])\hat{\sigma}_z \quad (16)$$

Last term is required to reproduce the correct Chern number and main features of perturbation spectrum:

$$C_{\pm} = \pm\frac{1}{2}(1 - sgn\left[J_2 m_{eff}\right]) \quad (17)$$

Finding: **additional symmetry-breaking nonlinear Bloch waves emerge which stability is sensitive to the band topology.**

References
[11] R. W. Bomanatara, W. Zhao, L. Zhou, J. Gong, Phys. Rev. B 96, 121406(R) (2017).

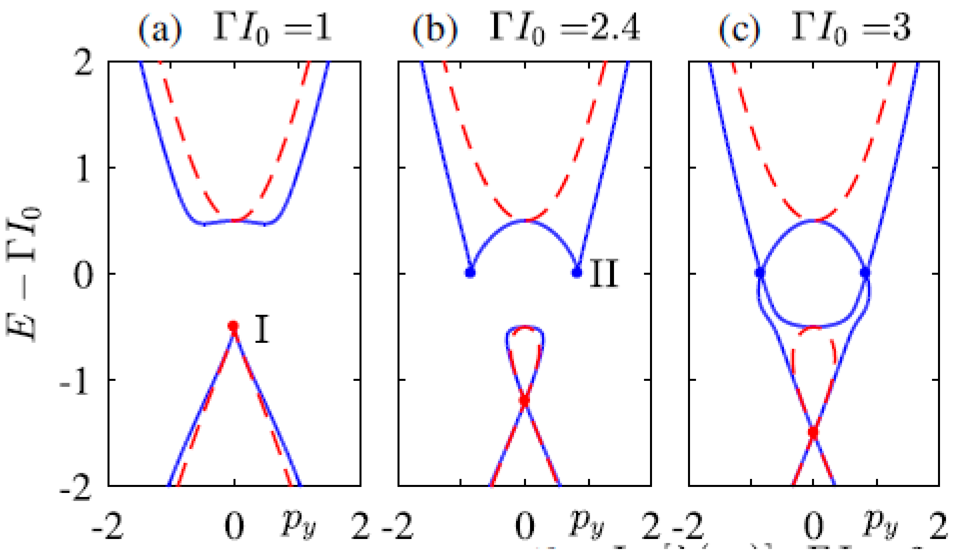

Fig. 5 Vicinity of critical line: nontrivial (blue, m_{eff}=-1/2) and trivial (red, m_{eff}=1/2); Dots – special points in spectra.

(a) I – *symmetry breaking bifurcation* $|p|=0$ *(* nl Dirac cone); *new mode emerges in both phases*
nontrivial phase –wave vectors perpendicular to the direction of the pseudospin remain stable;
trivial phase -- instability for all angles

(b) *II- nontrivial phase - additional bifurcation appears* ($C_\pm=\pm1$, $|\Delta/J_1|<2\sqrt{2}$) at $|p|=\sqrt{4-\Delta/J_2}$, $d_z(\mathbf{p})=0$ + *linear band crossing (loop) in both phases*

(c) *merging of new branches with the lower band* (nl provoked)→ gapless spectrum (nontrivial phase) vs. gapped (trivial phase)

AND: Trivial phase: pt modes maintain a similar polarization to the nl Bloch wave → efficient wave mixing
Nontrivial phase: poor overlapping of the nl Bloch wave and pt modes→ reduced nl mixing

MI depends on eigenvalue dispersion and is sensitive to band topology

(c) The long time dynamics: ***provided intra-band mixing***

Launched: nl Bloch wave (I_0), $\vec{k}_0 = (\pi, 0)$ + random pt (averaging – 100 initial pts) (32x32 cells)

Observables: - **participation numbers** P_r and P_k

$$P_r = \frac{\mathrm{P}^2}{2N}\left(\sum_r (|\psi_a(\vec{r})|^4 + |\psi_b(\vec{r})|^4)\right)^{-1} \tag{16}$$

-the **field polarization direction**: $\hat{\boldsymbol{n}}_\psi(\boldsymbol{k}) = \langle\psi(\boldsymbol{k})|\hat{\boldsymbol{\sigma}}|\psi(\boldsymbol{k})\rangle / \langle\psi(\boldsymbol{k})|\psi(\boldsymbol{k})\rangle$

Relative population imbalance: $n_z(\boldsymbol{k}) = (|\psi_a|^2 - |\psi_b|^2)/(|\psi_a|^2 + |\psi_b|^2)$

(17)

(18)

displays singularities sensitive to band topology (in the polarization azimuth)

~ Chern number ←→ $\theta = \frac{1}{2}\tan^{-1}(n_x/n_z)$

$\mathrm{sgn}(n_y)$ (19)

Averaged field polarization describes a mixed state with $n_\psi^2 = \langle\hat{\boldsymbol{n}}_\psi(\boldsymbol{k})\rangle \cdot \langle\hat{\boldsymbol{n}}_\psi(\boldsymbol{k})\rangle < 1$

(20)

-**purity gap:** $\min_k(n_\psi^2)$

Considered: ***exponential focusing, exponential defocusing. oscillatory defocusing regimes of instability***

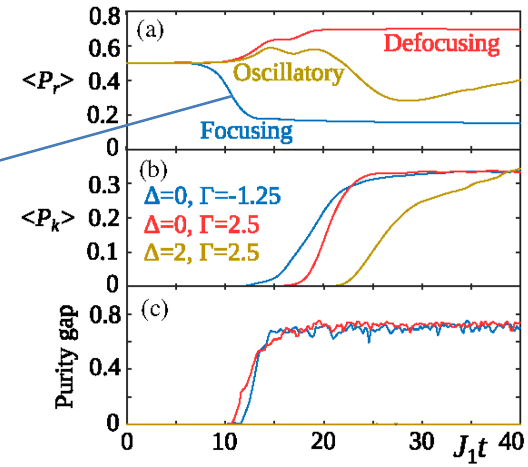

MI (exponential type) in focusing nl regime: $\Delta=0$, $\Gamma=-1.25$
Hamiltonians, total the configuration and Fourier space intensities

Soliton-like modes

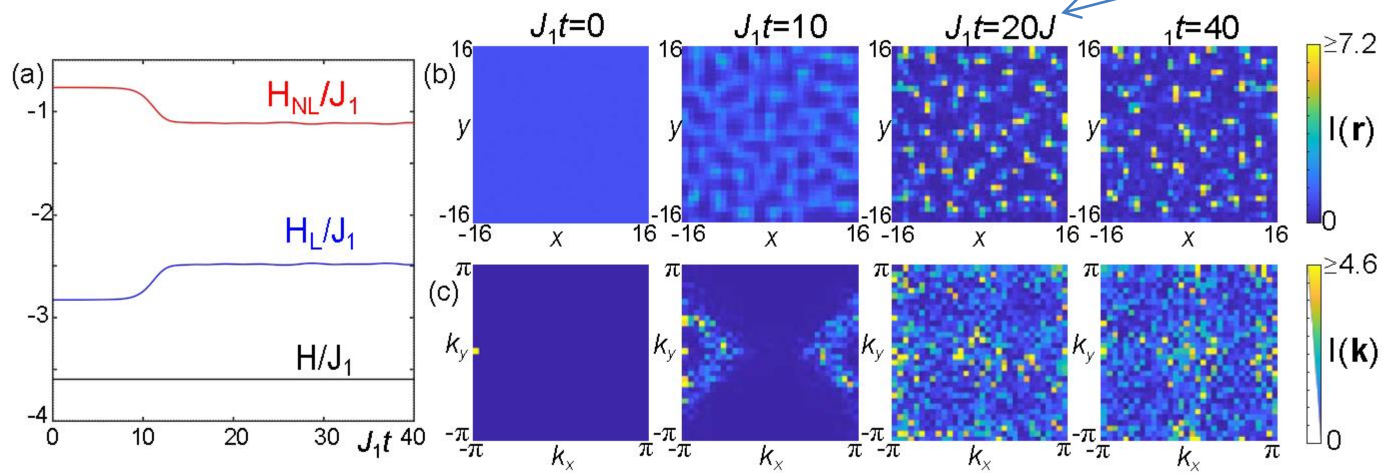

nl – wave mixing

Fig. 6

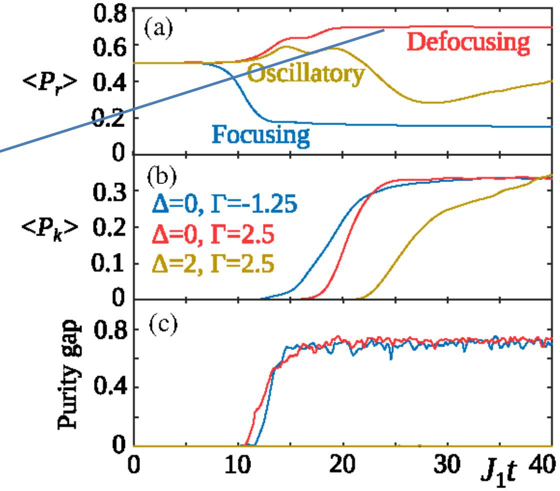

MI (exponentially type) in defocusing nl regime: $\Delta=0$, $\Gamma=2.5$

Absence of soliton-like modes

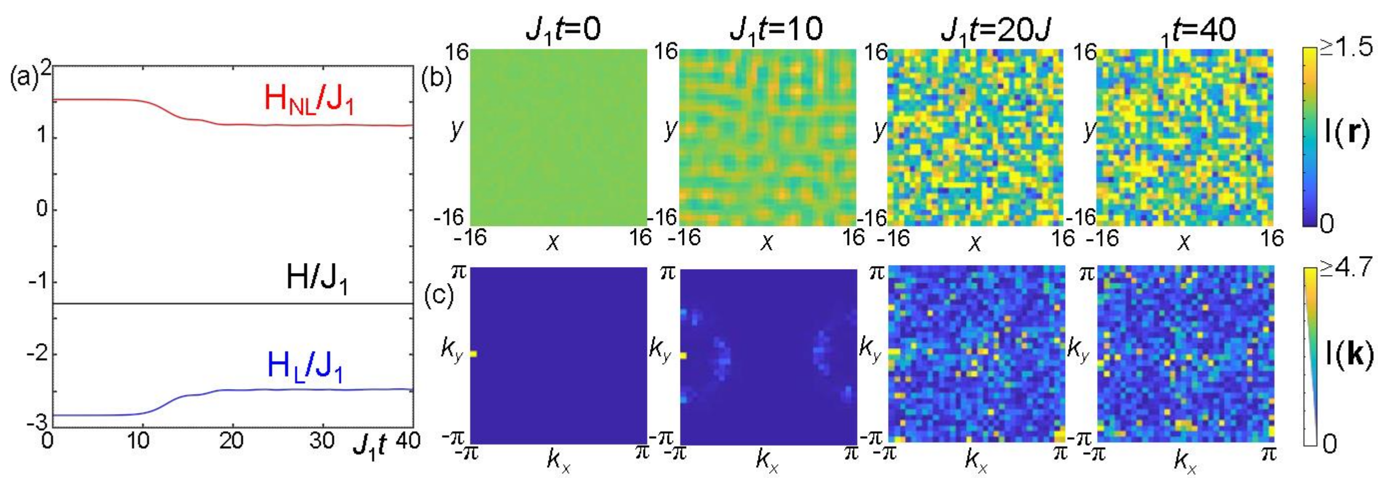

Fig. 7

nl – wave mixing

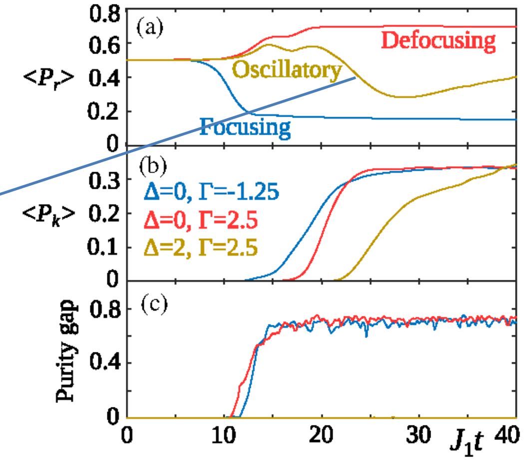

MI in the oscillatory instability regime: $\Delta=2$, $\Gamma=2.5$

Absence of stationary soliton-like structures

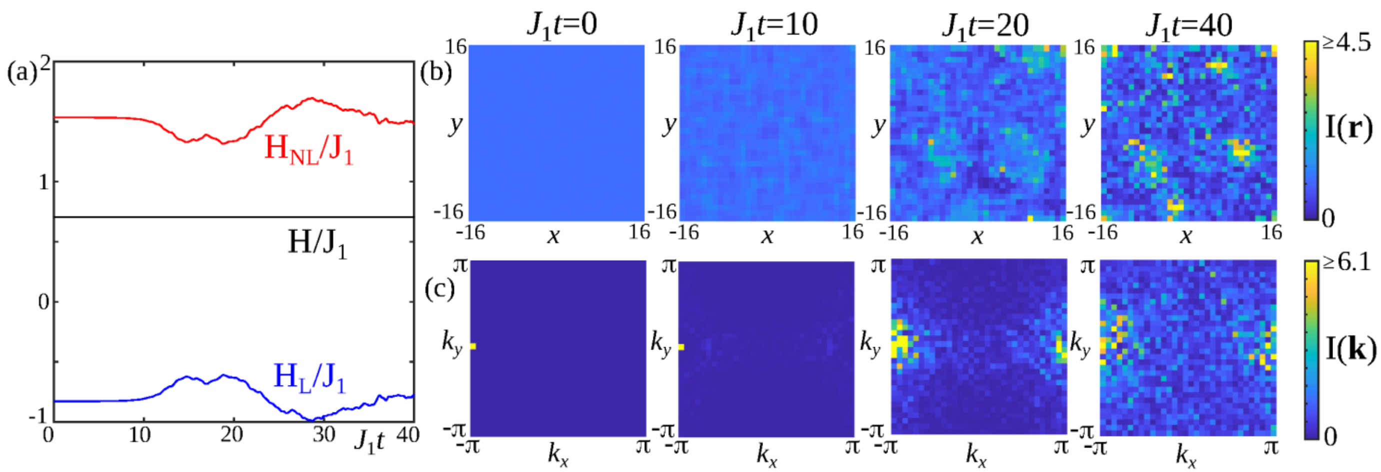

Fig. 8

nl – wave mixing

Intra-band wave mixing triggered by MI (weak nonlinearity or/and gapped bands)

Inter-band mixing (NL, gap width dependent)

Dynamics of the upper band population in different regimes $\int d\vec{k}\left|\langle u_{+}(\vec{k})|\psi(\vec{k},t)\rangle\right|^{2}$

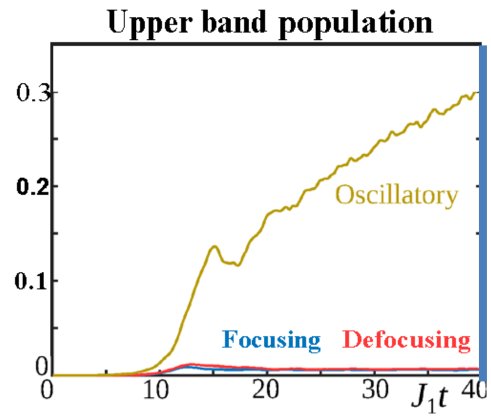

Fig. 10

Purity gap emergence vs. field polarization $\langle \hat{n}_{\psi}(\boldsymbol{k}) \rangle$

Trivial and nontrivial phases differ by field polarization :
Sum of charges of phase singularities of the polarization azimuth~ C
(b) Trivial , (c) nontrivial phase → Trivial C=0, nontrivial C=1.

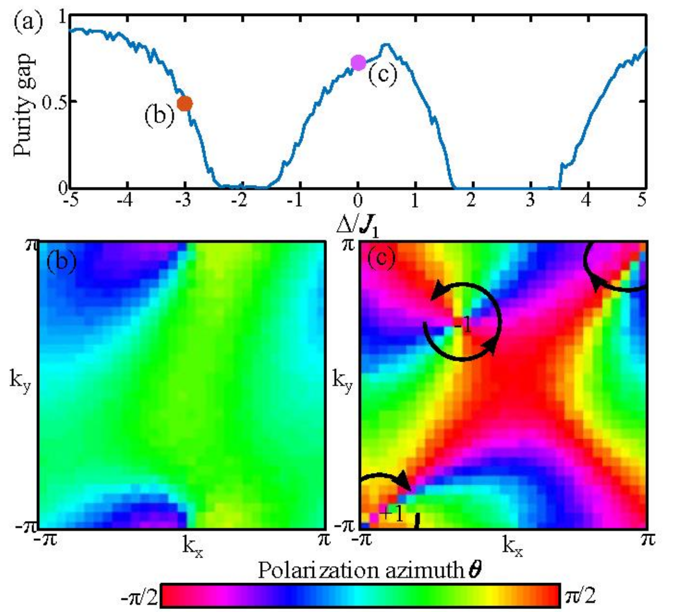

Fig. 9 Purity gap and field polarization at $t=40J_1$, $\Gamma=-2$
(b) Trivial phase ($\Delta=-3J_1$), *(c) nontrivial phase* ($\Delta=0$)

III **CONCLUSIONS:**

MI is sensitive to the geometrical properties of the Bloch waves,
i.e. their polarization

The long time instability dynamics can be used to measure the
band Chern number

The topological properties of the band are imprinted on the MI at small and large time and nonlinearity scales.

In progress:

Nonlinear wave mixing and relaxation (prethermalization/thermalization);
Can MI probe the band topology of Floquet lattices?